ACADEMIC PRESS

Available online at www.sciencedirect.com
SCIENCE DIRECT®

Journal of Catalysis 213 (2003) 7–16

JOURNAL OF CATALYSIS

www.elsevier.com/locate/jcat

Kinetics and modeling of 1-phenyl-1,2-propanedione hydrogenation

E. Toukoniitty, B. Ševčíková, P. Mäki-Arvela, J. Wärnå, T. Salmi, and D.Yu. Murzin *

Laboratory of Industrial Chemistry, Process Chemistry Group, Åbo Akademi, FIN-20500 Turku-Åbo, Finland

Received 21 February 2002; revised 3 June 2002; accepted 13 August 2002

Abstract

Kinetics and modeling of 1-phenyl-1,2-propanedione hydrogenation over cinchonidine-modified Pt/Al_2O_3 catalyst is reported. Hydrogenation experiments carried out in a pressurized autoclave (288 K, 1.2–6.5 bar hydrogen) revealed interesting kinetic effects which inspired the model development. The enantioselectivity towards the (*R*)-configuration, as well as the reaction rate and regioselectivity, depended on the modifier concentration having a maximum. The enantio- and regioselective effects were explained by the kinetic model, which assumes different number of sites for adsorption of the carbonyl groups of the 1-phenyl-1,2-propanedione as well as for the cinchonidine adsorbed in flat and tilted modes. The number of adsorption sites needed for the different species were obtained from molecular considerations and the hydrogenation rate constants were determined along with the adsorption parameters by non-linear regression analysis. A comparison of model predictions with experimental data revealed that the model accounts for the kinetic regularities.

Keywords: Hydrogenation; Diones; Enantioselectivity; Regioselectivity; Multicentered adsorption; Kinetic model

1. Introduction

Asymmetric hydrogenation over heterogeneous cinchona-alkaloid-modified Pt catalysts has received considerable attention and several attempts have been made to understand the mechanism of asymmetric induction [1–3]. Despite the significant progress made in surface-sensitive spectroscopic and quantum chemistry techniques, detailed kinetics is still a vital part of mechanistic studies. Kinetics provides information about prevailing reaction mechanisms and in connection with kinetic modeling offers a tool that allows comparison of proposed reaction mechanisms and can help in ruling out completely wrong mechanisms.

In contrast to well-investigated α-keto esters [1–3] with only one reactive center, hydrogenation of diones has received less attention [4,5]. In hydrogenation of asymmetric diones both enantio- and regioselectivity can be assessed. Asymmetric diones have two active prochiral carbonyl groups, which lead to two regioisomers upon addition of one hydrogen molecule as illustrated below:

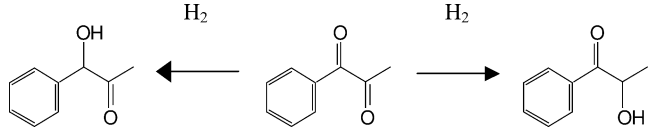

The regioisomers displayed above can exist both in (*R*)- and (*S*)-configurations, giving totally four different compounds as hydrogenation products. This implies that not only regioselectivity but also enantioselectivity aspects are involved.

Previously, interesting kinetic and selectivity aspects have been reported [9,10,13–15] in the hydrogenation of 1-phenyl-1,2-propanedione (**A** in Fig. 1) over cinchonidine-modified Pt catalysts, i.e., negligible rate acceleration in the presence of modifiers and high enantiomeric excess, $ee =$ 65% of the main product (*R*)-1-hydroxy-1-pnehylpropanone (**B**, in Fig. 1). However, systematic kinetic experiments have not been reported previously and, therefore, detailed kinetic experiments were carried out in the present work. The experiments were conducted in the absence of mass transfer limitations (both internal and external) at different reactant and modifier concentrations and hydrogen pressures.

The experiments revealed, e.g., that reaction rate and enantio- and regioselectivity exhibit a maximum around 1 : 1

* Corresponding author.
E-mail address: dmurzin@abo.fi (D.Yu. Murzin).

0021-9517/03/$ – see front matter
PII: S0021-9517(02)00025-8

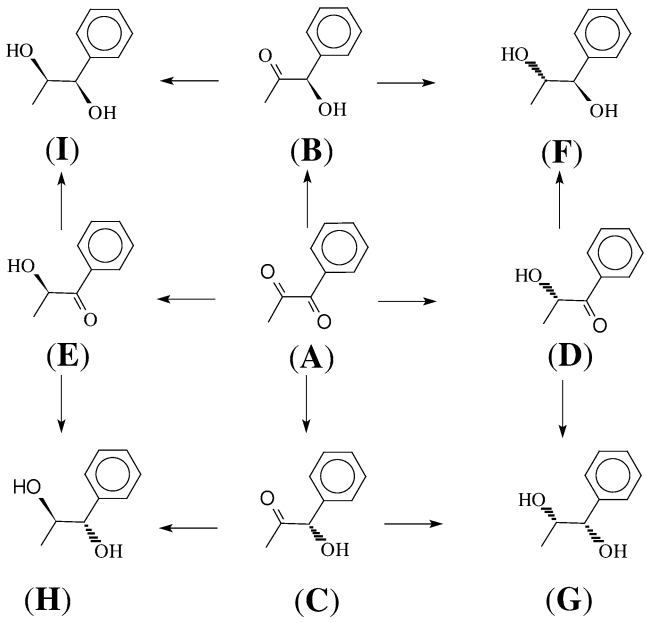

Fig. 1. Reaction scheme of 1-phenyl-1,2-propanedione hydrogenation. (**A**): 1-Phenyl-1,2-propanedione, (**B**): (*R*)-1-hydroxy-1-phenylpropanone, (**C**): (*S*)-1-hydroxy-1-phenylpropanone, (**D**): (*S*)-2-hydroxy-1-phenylpropanone, (**E**): (*R*)-2-hydroxy-1-phenylpropanone, (**F**): (1*R*,2*S*)-1-phenyl-1,2-propanediol, (**G**): (1*S*,2*S*)-1-phenyl-1,2-propanediol, (**H**): (1*S*,2*R*)-1-phenyl-1,2-propanediol, (**I**): (1*R*,2*R*)-1-phenyl-1,2-propanediol.

modifier-to-surface Pt ratio. Inspired by new observations reported in this work, kinetic modeling was carried out. Coverage-dependent adsorption modes, based on surface-sensitive infrared spectroscopy measurements, reported recently for cinchonidine [6–8], were used as a starting point in the kinetic modeling. The obtained results indicated that the coverage-dependent adsorption modes of cinchonidine account for the experimentally observed kinetic regularities.

2. Experimental section

2.1. Catalyst and chemicals

Commercial 5 wt% Pt/Al_2O_3 catalyst (Strem Chemicals, 78-1660) was used in the hydrogenation experiments. Catalyst characterization has been described in detail in our previous publications [9,10]. The main results from the catalyst characterization are summarized as follows: The metal content was 5 wt%, BET specific surface area 95 m^2/g, mean metal particle size 8.3 nm (XRD), dispersion 40% (H_2 chemisorption), and mean catalyst particle size 18.2 μm (Malvern).

The chemicals 1-phenyl-1,2-propanedione (Aldrich, 22303-4, 99%), ethyl acetate (Lab-Scan, A3511, 99.8%), and (−)-cinchonidine (Fluka, 27350, 98%) were used as received without further purification.

2.2. Reactor setup and experimental procedures

1-Phenyl-1,2-propanedione was hydrogenated in a pressurized batch reactor (Parr, 300 cm^3) equipped with an efficient turbine stirrer. The stirring velocity was 1000–1950 rpm. The hydrogen (AGA, 99.999%) pressure and temperature were 1.2–6.5 bar and 15 °C, respectively. A commercial 5 wt% Pt/Al_2O_3 catalyst was used. Typically, in the kinetic experiments, the catalyst mass and liquid volume were 0.15 g and 150 cm^3, respectively, and the stirring velocity was maintained at 1950 rpm. The catalyst was activated prior to the reaction under hydrogen flow (100 cm^3/min) for 2 h at 400 °C and cooled down to the reaction temperature.

An in situ modification procedure was adopted: the deoxygenated solution (10 min degassing in H_2 at atmospheric pressure), containing the solvent (ethyl acetate), the modifier (cinchonidine), and the substrate, was injected into the reactor, where the activated catalyst was under hydrogen and the reaction was commenced immediately. The modifier-to-catalyst mass ratio was from 1 : 150 to 120 : 150. The initial concentrations of 1-phenyl-1,2-propanedione and cinchonidine were varied between 0.01 and 0.025 mol dm^{-3} and 2.3×10^{-5} and 2.7×10^{-3} mol dm^{-3}, respectively.

2.3. Analytical procedure

Samples were withdrawn from the reactor at different time intervals and analyzed with a Varian 3300 gas chromatograph (GC) equipped with a chiral column (β-Dex 225; length 30 m, diameter 0.25 mm, film thickness 0.25 μm). Helium was used as a carrier gas with a split ratio of 33. The flame ionization detector and injector temperatures were 270 and 240 °C, respectively. The temperature program of the GC was 110 °C (30 min)—15 °C/min—250 °C (31 min). The details of synthesis of the compounds used for GC calibration and the assignment of the peaks are described in a previous publication [9].

3. Qualitative kinetics

In the following, the qualitative aspect of 1-phenyl-1,2-propanedione (**A**) hydrogenation kinetics over Pt/Al_2O_3 catalyst is presented. The complete reaction scheme of **A** hydrogenation is displayed in Fig. 1. The typical kinetic behavior is illustrated in Fig. 2. As can be seen, the consumption rate of **A** is relatively high compared to the rates of further reactions of hydroxyketones (**B** + **C** and **D** + **E**) to diols (**F**, **G**, **H**, and **I**). The kinetics was studied at different reactant (0.010–0.025 mol dm^{-3}) and catalyst-modifier (0–2.7×10^{-3} mol dm^{-3}) concentrations as well as at different hydrogen pressures (1.4–6.5 bar). The effect of temperature was outside of the scope of this work.

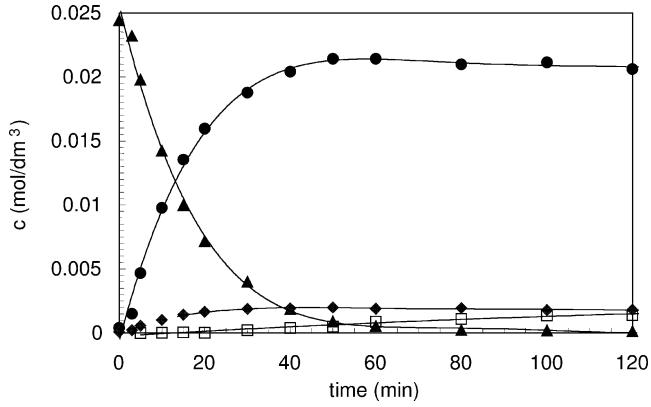

Fig. 2. Hydrogenation kinetics of 1-phenyl-1,2-propanedione in ethyl acetate at 15 °C. Catalyst: 5 wt% Pt/Al_2O_3 modified in situ with (−)-cinchonidine. Symbols: (▲) 1-phenyl-1,2-propanedione (**A**), (●) 1-hydroxy-1-phenylpropanone (**B** + **C**), (◆) 2-hydroxy-1-phenylpropanone (**D** + **E**), (□) 1-phenyl-1,2-propanediols (**F** + **G** + **H** + **I**).

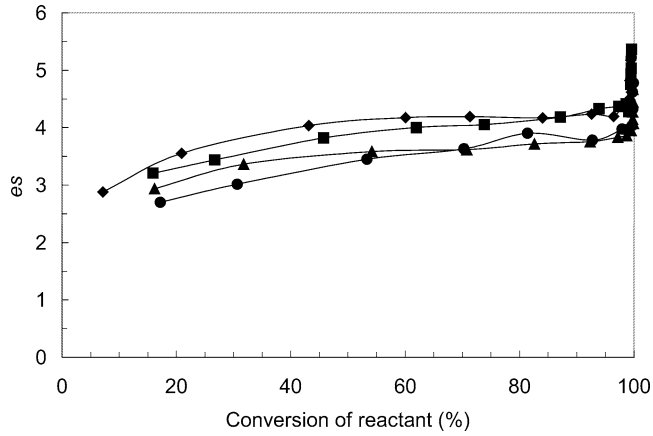

Fig. 3. Enantioselectivity (*es*) as a function of reactant conversion at different initial concentration of 1-phenyl-1,2-propanedione (**A**) at 6.5 bar H_2. Symbols: concentration of **A** (◆) 0.025 M, (■) 0.020 M, (▲) 0.015 M, (●) 0.010 M. Concentration of cinchonidine was 2.3×10^{-4} M.

3.1. Definitions of hydrogen uptake, regioselectivity, and enantioselectivity

The overall hydrogenation efficiency was expressed with the hydrogen uptake, $U(t)$ defined as

$$U(t) = \sum |\nu_i| c_i, \tag{1}$$

where $|\nu_i|$ is the stoichiometric coefficient of hydrogen added into the product molecule i and c_i denotes the concentration. The time derivative of $U(t)$ at $t = 0$ was taken as a measure of the initial hydrogenation rate. The regioselectivity (*rs*) is defined as the ratio between the concentrations of 1-hydroxy-1-phenylpropanone (**1-OH**) and 2-hydroxy-1-phenylpropanone (**2-OH**) and can be expressed as follows:

$$rs = \frac{[\mathbf{B}] + [\mathbf{C}]}{[\mathbf{D}] + [\mathbf{E}]} = \frac{[\mathbf{1\text{-}OH}]}{[\mathbf{2\text{-}OH}]}. \tag{2}$$

Enantioselectivity (*es*) is defined in analogy to regioselectivity,

$$es = \frac{[\mathbf{B}]}{[\mathbf{C}]}, \tag{3}$$

where [**B**] and [**C**] are the concentrations of (*R*)- and (*S*)-1-hydroxy-1-phenylpropanone, respectively (Fig. 1). For calculation of enantiomeric excess the following expression was used:

$$ee = \frac{[\mathbf{B}] - [\mathbf{C}]}{[\mathbf{B}] + [\mathbf{C}]} \times 100\%. \tag{4}$$

3.2. Verification of kinetic regime

The prerequisite for a proper kinetic experiment, i.e., working under a kinetic regime, was verified experimentally. The absence of external and internal mass transfer limitations was verified following commonly known procedures. In the experiments with different amounts of catalyst (0.050–0.40 g), a reaction rate proportional to the catalyst mass was observed. Furthermore, as the stirring velocity (1000–1950 rpm) was varied, a constant reaction rate was observed over a broad range using 0.150 g of the catalyst. The reactant and modifier concentrations were 0.025 and 2.3×10^{-4} mol dm^{-3}, respectively. These experiments were conducted at 15 °C and 6.5 bar H_2 pressure using the highest reactant concentration. The influence of internal mass transfer limitations has been evaluated in a previous publication for the same catalyst [9] and for the same reaction. The effectiveness factor (η_e) was found to be 0.94 under more severe conditions (higher c_A and T). Therefore, the effect of internal mass transfer limitations can be safely disregarded under the conditions employed in the present work. To summarize, the absence of external and internal mass transfer limitations was confirmed and further kinetic experiments were carried out under the kinetic regime using 0.15 g of catalyst and the highest agitation speed.

3.3. Effect of reactant concentration

The hydrogen uptake increased with increasing concentration of **A**. The reaction order with respect to the reactant was calculated from the estimated initial hydrogen uptakes obtained at different initial concentrations of **A**. The slope of a double logarithmic plot of the initial hydrogen uptake versus the concentration of **A**, gave a reaction order with respect to the reactant of 0.7, indicating the adsorption of **A** on the catalyst surface.

The regioselectivity was approximately constant ($rs =$ 10) as a function of the reactant concentration in the current experiments. Furthermore, the regioselectivity was constant also as a function of the reactant conversion up to a conversion level of 90%, but started then to increase due to the kinetic resolution of regioisomers.

The enantioselectivity increased slightly as the reactant concentration was increased (Fig. 3). The increase of enantioselectivity selectivity with increasing reactant con-

centration is in analogy with observations made with α-ketoesters [11], where both racemic and enantioselective hydrogenation exhibited a maximum as a function of reactant concentration. In the present work, due to low substrate concentrations, maxima in enantioselectivity were not yet reached and enantioselectivity increased as substrate concentration increased. The *es* increased also with increasing conversion of **A**, the initial *es* values at 10% conversion of **A** being ca. 30% less than at 90% conversion of **A**. Transient development of *ee* has been observed in α-keto ester hydrogenation; however, the transient period was obtained below 20% conversion of the reactant [12] after which *ee* reached a plateau. The further increase in *es* at high conversion levels (> 90%) was due to the kinetic resolution of **B** and **C**, analogously to the kinetic resolution of regioselectivity.

3.4. Effect of modifier concentration

The most pronounced effects on *es* and *rs* were observed when the modifier concentration was varied. Also the reaction rate depended on the modifier concentrations used. The reaction rate exhibited a maximum as the modifier concentration was increased (Fig. 4). A maximum rate acceleration of 30% with respect to the absence of modifier was observed at about 1 : 5 molar ratio of modifier-to-surface Pt. In the previous investigations [9,10,13–15], the maximum of the reaction rate at low modifier concentrations was not detected due to the non-optimized amounts of the modifier used. It can be noted that the maximum in enantioselectivity was observed at slightly higher modifier concentrations than the maximum in the hydrogenation rate. However, it still should be emphasized that both of the maxima appear relatively close to the 1 : 1 molar ratio of modifier to surface Pt and very far from the 1 : 1 ratio of modifier to reactant in the liquid bulk.

When the formation rates of **B** and **C** were examined, as a function of the modifier concentration, some interesting features emerged. In the absence of the modifier, the formation rates of **B** and **C** were equal resulting in a racemic mixture of **B** and **C**, as could be expected. However, when small amounts of modifier were introduced into the system the formation rate of **B** ((*R*)-enantiomer) rapidly increased and at the same time the formation rate of **C** ((*S*)-enantiomer) decreased significantly (Fig. 5). A maximum in the formation rate of **B** was observed at around 1 : 5 molar ratio of catalyst modifier-to-surface Pt, whereas maximum *es* was observed at slightly higher modifier concentrations corresponding to about 2 : 1 molar ratio of catalyst modifier to surface Pt (Fig. 6). After the observed maximum, the formation rate of **B** rate started to decrease as the modifier concentration was increased and the rate decreased at even much below the level observed in the absence of modifier (Fig. 5). Similar analysis for the formation of rate **C** revealed that the formation rate of **C** decreased rapidly when small amounts of modifier were present. As the amount of modifier was further increased, after the maximum enantioselectivity, the decrease in the formation rate of **C** was somewhat less pronounced. From these observations we conclude that

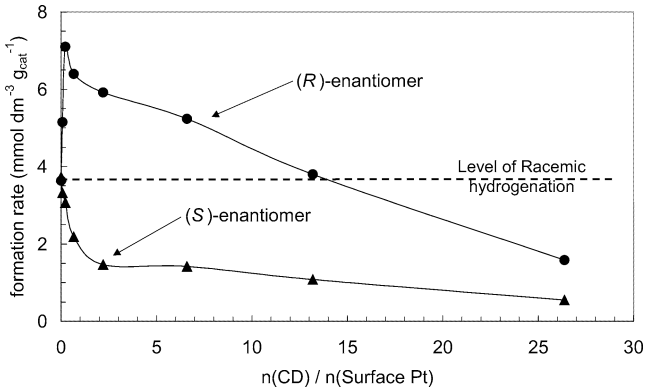

Fig. 5. Formation rates of (*R*)- and (*S*)-hydroxy-1-phenylpropanones at different molar rations of cinchonidine to surface Pt over 0.15 g of catalyst. The initial concentration of 1-phenyl-1,2-propandion and hydrogen pressure were 0.025 M and 6.5 bar, respectively.

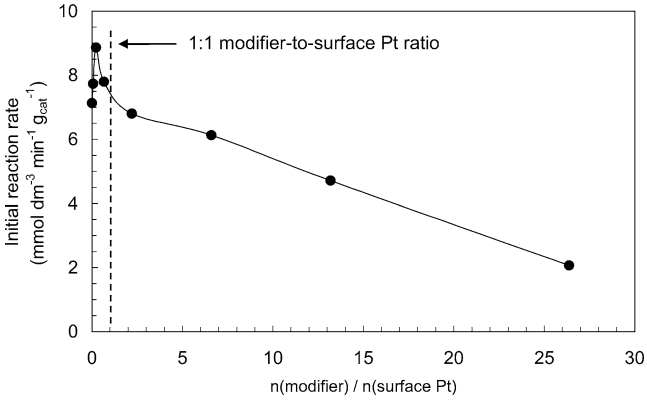

Fig. 4. The initial hydrogenation rate at different molar rations of cinchonidine-to-surface Pt over 0.15 g of catalyst. The concentration of 1-phenyl-1,2-propandion and hydrogen pressure were 0.025 M and 6.5 bar, respectively.

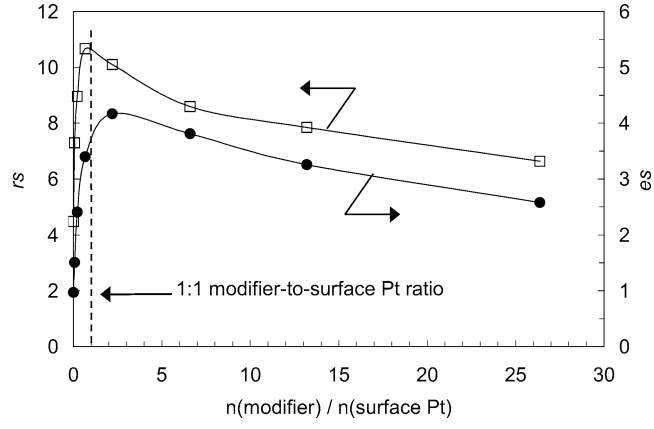

Fig. 6. Regioselectivity (*rs*) and enantioselectivity (*es*) in the hydrogenation of 1-phenyl-1,2-propanedione at different molar rations of cinchonidine-to-surface Pt over 0.15 g of catalyst. Symbols: (□) regioselectivity and (●) enantioselectivity.

up to a certain optimum value of the modifier concentration, the enantioselectivity and the reaction rate increase; however, a further increase in the modifier concentration results in a decreasing enantioselectivity and reaction rate. The explanation for the high enantioselectivity, $es = 4$ at max yield of **B** ($ee = 65\%$), is the increased formation rate of (*R*)-enantiomer promoted by the reduced formation rate of (*S*)-enantiomer in the presence of modifier.

3.5. Effect of hydrogen pressure

The effect of hydrogen pressure was found to be negligible as the hydrogen pressure was varied from 1.2 to 6.5 bar. The reaction order with respect to hydrogen was about zero over the studied pressure range. Neither *rs* nor *es* had any dependence on the hydrogen pressure. This indicates that hydrogen adsorption is mainly of a non-competitive nature. The role of hydrogen adsorption in the hydrogenation process is interesting: on the one hand, hydrogen is known to adsorb on Pt dissociatively and to compete on metal sites with organic molecules; on the other hand, hydrogen molecules are much smaller than the organic ones, particularly in the present case. Therefore in the present case it can be understood that interstitial sites between adsorbed organic molecules remain accessible for hydrogen adsorption and therefore, the adsorption behavior is shifted towards non-competitive behavior.

3.6. Consecutive hydrogenation to diols

According to the reaction scheme presented in Fig. 1, the primary products **B**, **C**, **D**, and **E** can be hydrogenated further to diols **F**, **G**, **H**, and **I**. The main product among the diols was (*R*,*S*)-1-phenyl-1,2-propanediol (**F**) in ethyl acetate as solvent. However, as can be seen from Fig. 2, the further reactions of the intermediates to diols were relatively slow and within the reaction times (3 h) used in this work the yield of diols remained low ($< 20\%$).

3.7. Phenyl ring hydrogenation

In the absence of the modifier, the phenyl ring in **A** was hydrogenated to a cyclohexyl ring; thus cyclohexyl products were formed both from the reactant and from all the products, giving in total eight cyclohexyl products. Generally it can be concluded that phenyl-ring hydrogenation was more favorable when there was more space on the catalyst surface for phenyl-ring adsorption and it only took place when there was no or a negligible amount of catalyst modifier. However, even in the absence of a modifier the yield of cyclohexyl derivatives remains low ($< 5\%$).

3.8. Discussion on qualitative kinetics

The pertinent kinetic regularities are discussed in more detail below, i.e., the lack of rate acceleration, the origin of enantioselectivity, and the maxima in selectivity (*es* and *rs*).

In the present study only negligible rate acceleration (30%) with respect to racemic hydrogenation was observed. Minor rate acceleration has been also reported in the hydrogenation of different α-substituted ketones [16]. The overall hydrogenation rate at highest enantio- and regioselectivity was lower than in the absence of catalyst modifier (Figs. 4 and 6). Therefore, in the light of present data it is evident that the origin of high enantioselectivity ($es = 4$, $ee = 65\%$) is not directly linked to the overall rate acceleration, but more precisely to the altered formation rates of the enantiomers in the presence of catalyst modifier. Analogous observation have been reported recently for ethylbenzoyl formate (EBF), which is the α-keto ester derivative of **A** [17]. In the hydrogenation of EBF *ee* of 98% was obtained, the enantioselective reaction being slower than the racemic hydrogenation, and it was put forward that rate acceleration is not a prerequisite for high enantioselectivity. Our experimental observations support the hypothesis that for good enantioselectivity overall rate acceleration is not necessarily needed, although it has commonly been observed using other substrates, e.g., ethyl and methyl pyruvates [1].

In the light of present data it is difficult to envisage that the liquid-phase substrate–modifier complex would be responsible for the enantioselectivity in the present case as assumed in the shielding effect model [18]. The maxima in selectivity near 1 : 1 modifier-to-surface Pt ratio (substrate-to-modifier ratio initially 370 : 1 in the liquid bulk) support that the enantiodifferentiating interaction occurs on the catalyst surface and not in the liquid bulk. Initially the liquid-phase composition comprises one substrate–modifier complex and 369 free reactant molecules and in the absence of overall rate acceleration negligible enantioselectivity would be observed in the framework of the shielding effect model, which assumes that enantiodifferentiation tales place exclusively in the liquid bulk. Therefore, we conclude that enantiodifferentiation of substrate–modifier interactions occur most probably on the catalyst surface under employed conditions as reasoned above.

The formation rate of **B** (*R*-enantiomer) is increased and exhibits a maximum, whereas the formation rate of **C** (*S*-enantiomer) is continuously decreasing as the modifier concentration is increased (Fig. 5). The increase of formation rate of **B** is a direct consequence of enantiodifferentiating interaction (ED) between substrate and modifier resulting in favorable formation of **B**. In the presence of modifier either the pro-B form (leading to **B** upon hydrogenation) reacts faster or the coverage of pro-B on the modified surface is higher due to the stabilizing ED interaction. An additional contributing factor is reduced surface area due to cinchonidine adsorption. Cinchonidine, being a bulky molecule, reduces the accessible active platinum surface as it adsorbs and should causes some deactivation with respect to racemic hydrogenation. In fact this was the case with the *S*-enantiomer, **C**. The formation rate of **C** continuously decreases as the modifier concentration was increased (Fig. 5). On the other hand, the formation rate of **B** in-

creased in the presence of cinchonidine and over a broad modifier concentration range the formation rate of **B** was higher than in the absence of modifier (Fig. 5). This cannot be simply accounted by the effect of reduced active surface, but more likely is a result of substrate–modifier interactions on the catalyst surface. The decrease in formation rate of **B** after the maximum can be a result of poisoning by adsorbed spectator species, which inhibit enantiodifferentiating substrate–modifier interaction. Adsorbed cinchonidine in parallel mode (active form) provides an enantioselective site and when the reactant is adsorbed in the vicinity, interaction between the reactant and the modifier leads to such an orientation that hydrogenation to forming **B** is preferred. However, when the tilted form of modifier (spectator) is adsorbed in the vicinity of actor species, the site becomes poisoned and the formation rate of **B** and the overall activity decrease.

The molecular-level substrate–modifier interactions have been discussed in detail in [3]. Two reaction routes have been proposed depending on the solvent used, where the pro-*R* substrate–modifier complex can be formed between protonated cinchonidine and **A** or alternatively between cinchonidine and the half-hydrogenated form of **A** [3]. The mechanism involving stabilization of the half-hydrogenated form of **A** would be more reasonable, because in ethyl acetate the modifier is not protonated and also in this scenario atomic hydrogen is added to the C=O double bond, which is formed via dissociative adsorption on H_2 on Pt.

The possible reasons for the maxima in selectivity and reaction rate can be explained in the light of recent findings concerning coverage dependent adsorption modes of cinchonidine [6–8]. At low coverage, cinchonidine adsorbs mainly via π-bonding of aromatic quinoline rings, the ring system being almost parallel to the metal surface. The adsorbed parallel form of the modifier would be involved in formation of enantiodifferentiation substrate–modifier complexes on the catalyst surface. At higher coverage, two additional tilted adsorption modes of cinchonidine were observed. The parallel and tilted adsorption modes of cinchonidine require different numbers of primary Pt sites for adsorption, the former occupying more active metal sites than the latter and being active in enantiodifferentiating interaction.

Therefore, with increasing cinchonidine coverage, the surface is occupied more by the ineffective form of the modifier and becomes unfavorable for the substrate–modifier interaction, thus lowering the selectivity. This would imply that after a certain optimum modifier coverage is reached, a further increase in the modifier concentration would result in a gradual decline in the *es* and *rs*. In a tilted adsorption mode, the catalyst surface accommodates more modifier onto it and less dione and as a result a lower reaction rate would be also observed. This would result in a maximum in *rs* and *es* as well as in reaction rate when the modifier concentration is increased. These observations are in accordance with current experimental results.

The coverage-dependent adsorption mode of the modifier is coupled with the coverage-dependent adsorption of the reactant as well. Over a nonmodified catalyst, the reactant can readily adsorb in a planar mode, where both of the carbonyl groups and the phenyl ring are in the same catalyst plane. This assumption is supported by the experiments, which revealed that the phenyl ring of **A** is hydrogenated in the absence of the modifier. The formed cyclohexyl products can be taken as an indication of a planar adsorption mode of the **A**, i.e., in order for the phenyl ring to be hydrogenated, it has to be adsorbed parallel to the catalyst surface via π-bonding. The mode of adsorption could be dependent on the concentration, as demonstrated recently [19] in selective hydrogenation of α,β-unsaturated aldehyde. It was supposed that the adsorption mode of cinnamaldehyde at high concentrations differs from that at lower concentrations; more precisely, cinnamaldehyde adsorbs at high concentrations perpendicular to the catalyst surface, with the aromatic rings in parallel arrangements. In our case, as small amounts of the modifier are added, the phenyl ring hydrogenation is no longer the preferential one, indicated by the disappearance of the cyclohexyl products. The adsorbed modifier occupies the surface in such a way that the planar adsorption of the reactant is no longer easy. This implies that the carbonyl groups are adsorbed at a somewhat tilted orientation. Therefore, the adsorption mode of the reactant also depends on the modifier coverage on the catalyst surface. The regioselectivity aspects would require two different adsorption modes for the reactant, because both carbonyl groups cannot adsorb simultaneously.

The same type of reasoning regarding the number of occupied sites could be applied also to substrate–modifier complexes.

The proposed mechanistic asumption are tested with the aid of kinetic modeling in the following.

4. Quantitative kinetics

4.1. Background

The quantitative treatment of the hydrogenation kinetics is based on the reaction scheme displayed in Fig. 1. Two adsorption modes of the modifier were selected for modeling, one mode being the parallel adsorbed species of cinchonidine involved in the enantiodifferentiation and the other being adsorbed in tilted mode only as a spectator on the catalyst surface. No discrimination between open and closed conformers of cinchonidine was made; however, it can be expected that the closed conformer also adsorbs in somewhat similar fashion and the steric constraints are similar to the open conformer. The conformation equilibrium of cinchonidine is mainly determined by the choice of solvent [20] and therefore, the varying conformational equilibria (open, closed) were left outside of the current work, as only ethyl acetate was used as solvent.

Two adsorption modes were used for the reactant as well, namely the adsorption of carbonyl groups 1 and 2, leading to regioselectivity.

In the present case, the role of hydrogen was discarded in the subsequent treatment due to the zero-order dependence on hydrogen, and the hydrogen adsorption parameters are invoked in the rate parameters.

The adsorption steps of the organic compounds are assumed to be rapid compared to the hydrogenation steps, which implies that quasi-equilibria are applied to the adsorption steps of the reactant (**A**) as well as the modifier (**M**). The adsorption of the product molecules is neglected. Only the first hydrogenation steps to **B**, **C**, **D**, and **E** (Fig. 1) are considered here, since the amount of diols formed was minor (Section 3.6) during the first stage of the experiments. For similar reasons the phenyl ring hydrogenation is discarded (Section 3.7). The hydrogenation steps are presumed to be irreversible and determine the rate of product formation.

4.2. Adsorption and hydrogenation steps

Based on the principles presented in the previous sections, the reaction mechanism is summarized as follows (vacant surface sites are denoted by *).

Adsorption of the reactant (**A**),

$$\mathbf{A} + m^* \rightleftharpoons \mathbf{A}1m^*, \tag{I}$$

$$\mathbf{A} + n^* \rightleftharpoons \mathbf{A}2n^*, \tag{II}$$

where $\mathbf{A}1m^*$ and $\mathbf{A}2n^*$ denote the adsorption modes of 1- and 2-carbonyls, respectively, and n, m the number of sites required for adsorption of them.

Adsorption of the modifier,

$$\mathbf{M} + p^* \rightleftharpoons \mathbf{M}p^*, \tag{III}$$

$$\mathbf{M} + q^* \rightleftharpoons \mathbf{M}q^*, \tag{IV}$$

where $\mathbf{M}p^*$ denotes the parallel adsorption mode of the cinchonidine involved in the enantiodifferentiating interaction with the adsorbed reactant $\mathbf{A}n^*$ or $\mathbf{A}m^*$. $\mathbf{M}q^*$ denotes the tilted adsorption mode of the cinchonidine, which adsorbs on the catalyst surface as a spectator.

Reactant–modifier interactions are assumed to be essential for transferring chirality to a prochiral reactant. Baiker [3] has discussed the mechanistic considerations for α-keto ester hydrogenation, from which it is reasonable to suppose that the site requirement for the substrate–modifier complex might be higher than the sum of the sites occupied by the reactant and the modifier separately.

Hence in the present kinetic treatment formation of substrate–modifier complexes is considered and they are assumed to be formed on the Pt sites in the following steps:

$$\mathbf{A}1m^* + \mathbf{M}p^* + f^* \rightleftharpoons \mathbf{A}1\mathbf{M}(mpf)^*, \tag{V}$$

$$\mathbf{A}2n^* + \mathbf{M}p^* + l^* \rightleftharpoons \mathbf{A}2\mathbf{M}(npl)^*. \tag{VI}$$

Here f and l are extra sites, which are required for the substrate–modifier complex to be formed compared to the site requirement for them separately.

Rigorous kinetic modeling in principle should include formation of half-hydrogenated species, which for racemic hydrogenation of the reactant on unmodified sites is described as

$$\mathbf{A}1m^* + \mathrm{H(ads)} \rightarrow \mathbf{A}1\mathbf{H}m^*, \tag{VII}$$

$$\mathbf{A}1\mathbf{H}m^* + \mathrm{H(ads)} \rightarrow 0.5\mathbf{B} + 0.5\mathbf{C} + m^* \tag{VIII}$$

and

$$\mathbf{A}2n^* + \mathrm{H(ads)} \rightarrow \mathbf{A}2\mathbf{H}n^*, \tag{IX}$$

$$\mathbf{A}2\mathbf{H}n^* + \mathrm{H(ads)} \rightarrow 0.5\mathbf{D} + 0.5\mathbf{E} + n^*. \tag{X}$$

As stated above, in the present treatment the role of hydrogen was discarded and the hydrogen adsorption parameters are invoked in the rate parameters.

Elementary reactions, which are summarized in Eqs. (VII)–(X), could be more complicated and are considered here as schematic representations, giving the correct stoichiometry of racemic hydrogenation.

Enantioselective hydrogenation of the reactant to (R)-enantiomer proceeds via reactions of the substrate–modifier complex,

$$\mathbf{A}1\mathbf{M}(mpf)^* + \mathrm{H(ads)} \rightarrow \mathbf{A}1\mathbf{M}\mathbf{H}(mpf)^*, \tag{XI}$$

$$\mathbf{A}1\mathbf{M}\mathbf{H}(mpf)^* + \mathrm{H(ads)} \rightarrow \mathbf{B} + m^* + p^* + f^* + \mathrm{M} \tag{XII}$$

and

$$\mathbf{A}2\mathbf{M}(npl)^* + \mathrm{H(ads)} \rightarrow \mathbf{A}2\mathbf{M}\mathbf{H}(npl)^*, \tag{XIII}$$

$$\mathbf{A}2\mathbf{M}\mathbf{H}(npl)^* + \mathrm{H(ads)} \rightarrow \mathbf{D} + n^* + p^* + l + \mathrm{M}. \tag{XIV}$$

In addition, some hydrogenation to (S)-enantiomers may take place on the modified sites. However, the contribution of these steps is easily obscured by the contributions of the racemic hydrogenation steps and was therefore, discarded in the present work.

4.3. Adsorption quasiequilibria

The use of the quasiequilibrium hypothesis for the adsorption steps (I)–(IV) implies that the concentrations of $\mathbf{A}1m^*$, $\mathbf{A}2n^*$, $\mathbf{M}p^*$, and $\mathbf{M}q^*$ are expressed by

$$c_{\mathbf{A}1m^*} = K_1 c_{\mathbf{A}} c^{*m}, \tag{5}$$

$$c_{\mathbf{A}2n^*} = K_2 c_{\mathbf{A}} c^{*n}, \tag{6}$$

$$c_{\mathbf{M}p^*} = K_3 c_{\mathbf{M}} c^{*p}, \tag{7}$$

$$c_{\mathbf{M}q^*} = K_4 c_{\mathbf{M}} c^{*q}. \tag{8}$$

If one also applies the quasiequilibrium hypothesis for the steps (V) and (VI), concentration of the complexes $\mathbf{A}1\mathbf{M}(mpf)^*$ and $\mathbf{A}2\mathbf{M}(npl)^*$ are expressed as

$$c_{\mathbf{A}1\mathbf{M}mpf^*} = K_5 c_{\mathbf{A}1m^*} c_{\mathbf{M}p^*} c^{*f} = K_1 K_3 K_5 c_{\mathbf{A}} c_{\mathbf{M}} c^{*m+p+f}, \tag{9}$$

$$c_{\mathbf{A}2\mathbf{M}npl^*} = K_6 c_{\mathbf{A}2n^*} c_{\mathbf{M}p^*} c^{*l} = K_2 K_3 K_6 c_{\mathbf{A}} c_{\mathbf{M}} c^{*n+p+l}. \tag{10}$$

Surface coverage of half-hydrogenated species could be computed applying quasi-steady state is assumptions; e.g.,

$$r_7 = r_8; \qquad r_9 = r_{10}; \qquad r_{11} = r_{12}; \qquad r_{13} = r_{14}, \tag{11}$$

leading to

$$c_{\mathbf{A1H}m^*} = k_7 c_{\mathbf{A}1m^*}/k_8, \tag{12}$$

$$c_{\mathbf{A2H}n^*} = k_9 c_{\mathbf{A}2m^*}/k_{10}, \tag{13}$$

$$c_{\mathbf{A1MH}mpf^*} = k_{11} c_{\mathbf{A1M}mpf^*}/k_{12}, \tag{14}$$

$$c_{\mathbf{A2MH}npl^*} = k_{13} c_{\mathbf{A2M}npl^*}/k_{14}. \tag{15}$$

All these expressions are inserted in to the total balance of metal sites,

$$\begin{aligned} &m(1 + k_7/k_8)c_{\mathbf{A}1m^*} + n(1 + k_9/k_8)c_{\mathbf{A}2n^*} + pc_{\mathbf{M}p^*} + qc_{\mathbf{M}q^*} \\ &\quad + mpf(1 + k_{11}/k_{12})c_{\mathbf{A1M}mpf^*} \\ &\quad + npl(1 + k_{13}/k_{14})c_{\mathbf{A2M}npl^*} + c^* = c_0, \end{aligned} \tag{16}$$

where c_0 and c^* denote the total concentration of accessible sites and the concentration of vacant sites, respectively.

After inserting the quasi-equilibria into the total balance of sites, coverage of all species can be expressed *via* the fraction of vacant sites, $\Theta = c^*/c_0$:

$$\begin{aligned} &c_{\mathbf{A}}\left(mK_1(1 + k_7/k_8)c_0^{(m-1)}\Theta^m + nK_2(1 + k_9/k_8)c_0^{(n-1)}\Theta^n\right) \\ &\quad + c_{\mathbf{M}}\left(pK_3c_0^{(p-1)}\Theta^p + qK_4c_0^{(q-1)}\Theta^q\right) \\ &\quad + (m + p + f)K_1K_3K_5(1 + k_{11}/k_{12}) \\ &\qquad \times c_{\mathbf{A}}c_{\mathbf{M}}c_0^{(m+p+f-1)}\Theta^{m+p+f} \\ &\quad + (n + p + l)K_2K_3K_6(1 + k_{13}/k_{14}) \\ &\qquad \times c_{\mathbf{A}}c_{\mathbf{M}}c_0^{(n+p+l-1)}\Theta^{n+p+l} \\ &\quad + \Theta = 1. \end{aligned} \tag{17}$$

At the present stage, the following combination of parameters is wise: $K_1' = mK_1(1 + k_7/k_8)c_0^{(m-1)}$, $K_2' = nK_2(1 + k_9/k_8)c_0^{(n-1)}$, $K_3' = pK_3c_0^{(p-1)}$, $K_4' = qK_4c_0^{(q-1)}$, $K_5' = (m + p + f)K_1K_3K_5(1 + k_{11}/k_{12})c_0^{(m+p+f-1)}$, $K_6' = (n + p + l)K_2K_3K_6(1 + k_{13}/k_{14})c_0^{(n+p+l-1)}$. Consequently, the site balance obtains a very convenient form

$$\begin{aligned} f(\Theta) &= c_{\mathbf{A}}\left(K_1'\Theta^m + K_2'\Theta^n\right) + c_{\mathbf{M}}\left(K_3'\Theta^p + K_4'\Theta^q\right) \\ &\quad + c_{\mathbf{A}}c_{\mathbf{M}}\left(K_5'\Theta^{m+p+f} + K_6'\Theta^{n+p+l}\right) + \Theta - 1 = 0. \end{aligned} \tag{18}$$

4.4. Hydrogenation rates

The rates of the hydrogenation steps (VII), (IX) and (XI), (XIII) are expressed as follows:

$$r_7 = k_7 c_{\mathbf{A}1^*}, \tag{19a}$$

$$r_9 = k_9 c_{\mathbf{A}2^*}, \tag{19b}$$

$$r_{11} = k_{11} c_{\mathbf{A1M}^*}, \tag{19c}$$

$$r_{13} = k_{13} c_{\mathbf{A2M}^*}. \tag{19d}$$

It should be borne in mind that the rate constants de facto include the effect of hydrogen concentration, which in our case remained invisible. For practical purposes, the rate expressions are compressed to

$$r_7 = k_7' c_{\mathbf{A}}\Theta^m, \tag{20a}$$

$$r_9 = k_9' c_{\mathbf{A}}\Theta^n, \tag{20b}$$

$$r_{11} = k_{11}' c_{\mathbf{A}}c_{\mathbf{M}}\Theta^{m+p+f}, \tag{20c}$$

$$r_{13} = k_{13}' c_{\mathbf{A}}c_{\mathbf{M}}\Theta^{n+p+l}, \tag{20d}$$

where the combined parameters (k') contain the rate constants (k), the equilibrium constants (K), and the total concentration of sites (c_0).

4.5. Component generation rates and mass balances

The generation rates of the compounds are obtained from the stoichiometric scheme (Fig. 1)

$$r_{\mathbf{A}} = -(r_7 + r_9 + r_{11} + r_{13}), \tag{21a}$$

$$r_{\mathbf{B}} = 0.5r_7 + r_{11}, \tag{21b}$$

$$r_{\mathbf{C}} = 0.5r_7, \tag{21c}$$

$$r_{\mathbf{D}} = 0.5r_9 + r_{13}, \tag{21d}$$

$$r_{\mathbf{E}} = 0.5r_9. \tag{21e}$$

The generation rates are combined with the mass balances of the components. Here we assume that the volatilities of the organic components are negligible and thus it is enough to consider the liquid phase only. The balance equations become

$$\mathrm{d}c_i/\mathrm{d}t = \rho_{\mathrm{B}} r_i, \tag{22}$$

where $i = \mathbf{A}, \mathbf{B}, \ldots, \mathbf{E}$ and ρ_{B} is the mass-of-catalyst-to-liquid-volume ratio.

4.6. Parameter estimation procedure

For parameter estimation purposes primary concentration vs time data from 12 experiments were used. The data at different hydrogen pressures were not used in estimation due to zero-order dependence on hydrogen. The fraction of vacant sites (Θ) was calculated in situ from the balance Eq. (18) during the estimation of kinetic parameters. The non-linear equation was solved using previously demonstrated numerical approach [21]. The balance equation was solved by Newton's method, i.e., $\Theta_{(k+1)} = \Theta_{(k)} - f(\Theta_{(k)})/f'(\Theta_{(k)})$, where f' is the derivative of f, while k denotes the iteration index. Parameters m, n, p, q, l, and f were estimated by data fitting. An initial estimate of $\Theta = 0.01$ was used at the very beginning of the parameter estimation. Later on, a previously converged value of Θ was utilized to start a new iteration cycle.

The residual sum of squares (Q) was minimized during the parameter estimation,

$$Q = \sum (c_{i,t\,(\mathrm{model})} - c_{i,t\,(\mathrm{exp})})^2, \tag{23}$$

where the subscripts i and t refer to components and the corresponding times, respectively. For compounds **D** and **E** a lumped concentration was used in the parameter estimation. The model predictions were obtained by solving the differential Eq. (15) (ODEs) for all of the components (**A**, ..., **E**) during the parameter estimation. A stiff ODE solver [22] was used to guarantee a rapid and stable solution. The residual sum of squares was minimized by a combined simplex–Levenberg–Marquardt algorithm implemented in the software Modest [23]. The minimization was commenced by the simplex algorithm, but was switched to the more rapid Levenberg–Marquardt algorithms as the minimum was approached.

4.7. Results from parameter estimation

Estimated parameter values and estimation results are collected in Table 1, which shows relatively good statistics on the estimated parameters. Their standard errors are within reasonable limits, except for reactions, which are of secondary importance. The correlation matrix for the estimated parameters is given in Table 2. Examples of the fit are provided in Fig. 7, which shows very good agreement between the experimentally recorded and the predicted concentrations.

It turned out that some adsorption equilibrium constants (K'_1, K'_2, and K'_6) could not be reliably obtained from the parameter estimation. This is understandable, because in the site balance equation the contribution of them with respect to K'_3 and K'_4 might be minor, due to the large adsorption equilibrium constants of modifier.

In addition, it is important to note that as the model was able to predict the concentration vs time behavior of all components (Fig. 7), it can also account for the *es* and *rs* dependency on modifier and reactant concentrations, as the

Table 1
Kinetic and adsorption parameters obtained from parameter regression[a]

Parameter	Value	Units	Relative error, %
M	2.15		11
N	1.8		21
P	3.2		12
q	0.3		60
f	0.55		13
l	0.48		>100
K'_1	4.1	$\mathrm{L\,mol^{-1}}$	43
K'_2	1.4	$\mathrm{L\,mol^{-1}}$	89
K'_3	2780	$\mathrm{L\,mol^{-1}}$	12
K'_4	283	$\mathrm{L\,mol^{-1}}$	28
K'_5	20.2	$\mathrm{L^2\,mol^{-2}}$	27
K'_6	0.16	$\mathrm{L^2\,mol^{-2}}$	>100
k'_7	62	$\mathrm{L\,s^{-1}\,g_{cat}^{-1}}$	5.3
k'_9	10.9	$\mathrm{L\,s^{-1}\,g_{cat}^{-1}}$	8.6
k'_{11}	0.13×10^7	$\mathrm{L^2\,s^{-1}\,g_{cat}^{-1}}$	11.8
k'_{13}	0.12×10^5	$\mathrm{L^2\,s^{-1}\,g_{cat}^{-1}}$	>100

[a] Degree of explanation: 97.55%.

Table 2
Correlation matrix of parameters

	q	p	n	m	f	l	K_1	K_2	K_3	K_4	K_5	K_6	k_7	k_9	k_{11}	k_{13}
q	1															
p	−0.597	1														
n	−0.259	0.563	1													
m	−0.555	0.794	0.618	1												
f	−0.347	0.440	0.429	0.636	1											
l	−0.021	−0.119	−0.76	−0.16	−0.12	1										
K_1	−0.244	0.239	0.089	0.443	0.552	0.342	1									
K_2	−0.147	0.132	0.025	0.088	0.023	−0.20	−0.68	1								
K_3	−0.411	0.364	−0.145	−0.136	−0.172	0.184	−0.20	0.086	1							
K_4	0.971	−0.671	−0.385	−0.718	−0.472	0.044	−0.301	−0.169	−0.293	1						
K_5	0.635	−0.880	−0.614	−0.888	−0.690	0.171	−0.344	−0.265	−0.113	0.752	1					
K_6	0.052	0.023	0.027	0.222	0.348	0.084	0.669	−0.523	−0.352	0.018	−0.093	1				
k_7	−0.492	0.528	0.277	0.828	0.652	0.159	0.614	−0.013	−0.210	−0.623	−0.713	0.335	1			
k_9	−0.299	0.451	0.557	0.559	0.488	0.273	0.077	−0.229	−0.125	−0.394	−0.551	0.176	0.387	1		
k_{11}	−0.506	0.829	0.266	0.567	0.485	0.096	0.246	0.081	0.621	−0.547	−0.722	−0.005	0.414	0.300	1	
k_{13}	0.035	−0.075	−0.451	−0.155	−0.141	0.757	0.533	−0.568	0.194	0.083	0.157	−0.011	0.087	−0.436	0.090	1

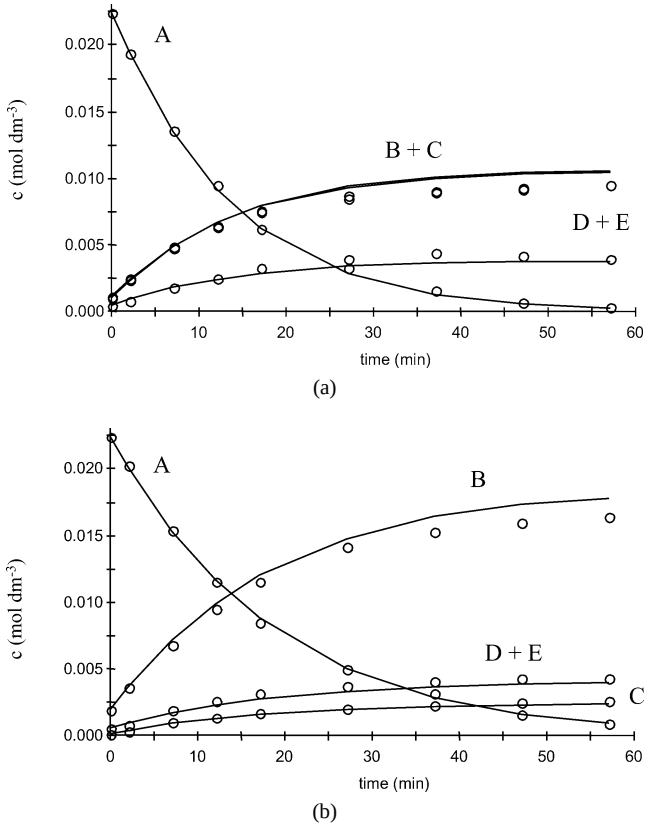

Fig. 7. The comparison of the model predictions (solid line) with experimental data (open circles) at 6.5 bar H_2 over 0.15 g of catalyst. Conditions: (a) racemic hydrogenation, $c_{\mathbf{A}} = 0.025$ M, (b) $c_{\mathbf{M}} = 6.8 \times 10^{-4}$ M, $c_{\mathbf{A}} = 0.025$ M.

primary c vs t data are used also in calculations *es* and *rs*. However, some deviations at high conversion are visible. A possible explanation for such behavior is that kinetic resolution was not accounted for by the model as only the first reaction steps were considered and the further reactions to diols were discarded.

5. Conclusions

Kinetics of 1-phenyl-1,2-propanedione (**A**) over modified Pt was studied in the absence of mass transfer limitations. The reaction had negligible rate acceleration in presence of cinchonidine and ee of 65% ($es = 4$) of the main product could be obtained. Enantio- and regioselectivity exhibited a maximum around 1 : 1 cinchonidine-to-modifier molar ratio. Reaction order was found to be about zero order with respect to hydrogen.

A new kinetic model was developed for enantioselective hydrogenation of 1-phenyl-1,2-propanedione (**A**) over modified Pt in order to explain the kinetic regularities. As a basis for the model development different adsorption modes of the carbonyl groups of the reactant as well as the parallel and tilted adsorption modes of the modifier were used. This approach reflects the coverage dependent adsorption of the reactant and the modifier, leading to the changes of the enantioselectivity and regioselectivity as a function of the reactant and modifier concentrations. The model also took into account formation of the surface–modifier complexes. The model explained the essential features of enantioselective hydrogenation of 1-phenyl-1,2-propanedione (**A**) and would be useful in the future in kinetic modeling of other heterogeneous catalytic reactions involving complex organic molecules too.

Acknowledgments

This work is part of the activities at the Åbo Akademi Process Chemistry Group within the Finnish Centre of Excellence Programme (2000–2005) of the Academy of Finland. Financial support from the Finnish Graduate School in Chemical Engineering (GSCE) is gratefully acknowledged. The unknown referee is acknowledged for numerous suggestions, which helped to improve the manuscript.

References

[1] M. von Arx, T. Mallat, A. Baiker, Top. Catal. 19 (2002) 75, and references therein.
[2] A. Baiker, J. Mol. Catal. A Chem. 115 (1997) 473.
[3] A. Baiker, J. Mol. Catal. A Chem. 163 (2000) 215.
[4] J. Slipszenko, S. Griffiths, P. Johnston, K. Simons, W. Vermeer, P. Wells, J. Catal. 179 (1998) 267.
[5] M. Studer, V. Okafor, H.U. Blaser, Chem. Commun. (1998) 1054.
[6] D. Ferri, T. Bürgi, J. Am. Chem. Soc. 123 (2001) 12074.
[7] D. Ferri, T. Bürgi, A. Baiker, Chem. Commun. (2001) 1172.
[8] J. Kubota, F. Zaera, J. Am. Chem. Soc. 123 (2001) 11115.
[9] E. Toukoniitty, P. Mäki-Arvela, M. Kuzma, A. Villela, A. Kalantar Neyestanaki, T. Salmi, R. Sjöholm, R. Leino, E. Laine, D.Yu. Murzin, J. Catal. 204 (2001) 281.
[10] E. Toukoniitty, P. Mäki-Arvela, A. Nunes Villela, A. Kalantar Neyestanaki, R. Leino, T. Salmi, R. Sjöholm, E. Laine, J. Väyrynen, T. Ollonqvist, P.J. Kooyman, Catal. Today 60 (2000) 175.
[11] H.-U. Blaser, H.-P. Jalett, M. Garland, M. Studer, H. Thies, A. Wirth-Tijani, J. Catal. 173 (1998) 282–294.
[12] J. Wang, Y. Sun, C. LeBlond, R.N. Landau, D.G. Blackmond, J. Catal. 161 (1996) 752.
[13] E. Toukoniitty, P. Mäki-Arvela, A. Kalantar Neyestanaki, T. Salmi, A. Villela, R. Leino, R. Sjöholm, E. Laine, J. Väyrynen, T. Ollonqvist, Stud. Surf. Sci. Catal. 130 (2000) 3363.
[14] E. Toukoniitty, P. Mäki-Arvela, J. Wärnå, T. Salmi, Catal. Today 66 (2001) 411.
[15] E. Toukoniitty, P. Mäki-Arvela, A. Kalantar Neyestanaki, T. Salmi, R. Sjöholm, R. Leino, E. Laine, P.J. Kooyman, T. Ollonqvist, J. Väyrynen, Appl. Catal. A Gen. 216 (2001) 73.
[16] A. Vargas, T. Bürgi, M. von Arx, R. Hess, A. Baiker, J. Catal. 209 (1996) 489.
[17] M. Sutyinszki, K. Szöri, K. Felföldi, M. Bartok, Catal. Commun. 3 (2002) 125.
[18] J. Margitfalvi, E. Hegedus, E. Tfirst, Tetrahedron Asymmetry 7 (1996) 571.
[19] R.J. Berger, E.H. Stitt, G.B. Marin, F. Kapteijn, J.A. Moulijn, CATTECH 5 (2001) 30.
[20] T. Bürgi, A. Baiker, J. Am. Chem. Soc. 120 (1998) 12920.
[21] L.P. Lindfors, T. Salmi, IEC Res. 32 (1993) 34.
[22] A. Hindmarsh, in: Scientific Computing, Vols.55–64, IMACS, Amsterdam, 1982.
[23] H. Haario, Modest 6.0—A User's Guide, ProfMath, Helsinki, 2001.